Geometrically non-linear analysis of composite shells under uniform thermal loading

Agnieszka Sabik[1] **and Ireneusz Kreja**[1]*

[1]*Department of Structural Mechanics and Bridge Structures, Gdansk University of Technology*
ul. Narutowicza 11/12, 80-233 Gdańsk, Poland
e-mail: agsa@pg.gda.pl

Abstract

The paper deals with a geometrically non-linear analysis of multilayered composite panels subjected to uniform thermal loading. The main goal of the analysis is to estimate the load capacity of a structure taking into account the loss of stability and the strength limit. As a representation of multilayered composite medium the *Equivalent Single Layer* approach with the linear displacement field in the thickness direction of a shell and non-zero transverse shear strains has been adopted. All computations have been performed with the use of an isoparametric doubly-curved shell elements implemented in the authors' own FEM-code.

Keywords: shells, laminates, stability, large deformations, numerical analysis

1. Introduction

Among all useful advantages, like a high strength-to-weight ratio or good chemical resistance, superior thermal insulation parameters are one of the most remarkably characteristics of composite materials. For that reasons in the beginning they have been extensively used in the aeronautics and aerospace industry as fuselages or turbine blades in jet engines. Nowadays multilayered composite shells can be found in many other branches of industry, serving as carrying members or covers of various constructions. One can mention here several examples as: wind turbine blades, underwater vehicles, bicycles, additional reinforcement of concrete structures or industrial chimneys [5].

The objective of this work is to predict the limit load level of composite shells subjected only to a uniform temperature rise. Due to the typical slenderness of composite structures, one should consider not only the stress bearing capacity, but also the problem of shell stability.

In the present study the buckling load level is estimated on a basis of the geometrically non-linear incremental analysis, whereas stress state is monitored according to the Tsai-Wu failure criterion, see e.g. [8].

2. Theoretical model

A multilayered composite shell represents a non-homogenous medium, in which an every layer is usually by itself also non-homogenous as well as non-isotropic. From this point of view, the most suitable models for its representation appear to be the three-dimensional approaches. Taking into account, that during the 3D finite element modelling, there should be used at least one brittle element per thickness of each layer, such formulations are numerically very expensive, if the complete structure is to be analysed. Therefore, in practice an application of 3-D approaches is reasonable only for a detailed analysis of limited "special care" regions as for example cut-outs edges where stress concentration takes place [16]. With regard to this limitations of the 3-D analysis a great number of two-dimensional models have been developed during the last decades. One can distinguish two main groups of these formulations, namely the Discrete Layer (*DL*) (sometimes called layer-wise [2]) models or the Equivalent Single Layer approaches (*ESL*) [2, 11].

ESL models can be considered as a simple adaptation of the well established 2-D formulations known from the analysis of isotropic, homogeneous plates and shells. The whole laminate is modelled here as only one layer with an equivalent stiffness of the multilayered cross-section. This stiffness comes out straightforward from the analogous integration as that used for the computation of resultant forces on the base of stresses. In the finite element modelling within the framework of *ESL* formulations the number of degrees of freedom is independent of the number of layers.

The *DL* models present an in-between approach or a kind of compromise if compared with 3-D and *ESL* formulations. In *DL* models each layer is considered as a two-dimensional medium with own reference surface. The presence and influence of other layers are enclosed in various continuity assumptions at layer-interfaces [2, 11]. Obviously *DL* models are more accurate than *ESL* formulations, but in this case the number of degrees of freedom depends on the number of layers, thus the computational cost of using *DL* approach can be relatively high, especially if nonlinear phenomena are analysed.

In the present study the *ESL* approach is adopted. As stated before, the resulting two-dimensional model of a layered shell can base on one of the theories established for homogeneous isotropic shells. The simplest 2-D formulation is the Classical Lamination Theory (*CLT*) which refers to the Kirchhoff shell theory [8]. However, due to the basic assumption of neglected transverse shear strains, *CLT* formulations are rather inappropriate for modelling of shells made of composites, because of the significant shear compliance of these materials. Thus, various types of shear-theories have been extended for analysis of multilayered shells [11, 15, 16].

In the current formulation the First Order Shear Deformation Theory (*FOSD*) [10] is applied. In the most common displacement formulation of finite elements its essential assumption of the straight but not necessarily normal line makes the using of appropriate shear correction necessarily. For laminated medium it is rather inconvenient to apply a pre-defined value of shear factor, like it is usually made in case of homogeneous shells [4]. More accurate for laminated bodies seem to be shear factors or even the shear stiffness matrix evaluated numerically for the entire cross-section. It must be

* This work was partly financed by the Polish Ministry of Science and Higher Education as the research project no. N N506 254237.

stressed, that such a method requires some basic presumptions. Very often, the foundation for such an approach is an assumption of a cylindrical bending mode [20]. In the authors' opinion, this technique is very efficient due to its accuracy and simplicity [17], therefore it is applied also in the present approach.

3. Incremental formulation

All presented here computations have been performed with the use of authors' own FEM-code programmed in Fortran.

As mentioned earlier, the limit load level for a shell structure can strongly depend on the stability aspects, therefore an incremental large displacement analysis should be carried out. The linearized incremental equilibrium equation for the temperature load in a standard matrix notation states:

$$ {}_0^1\mathbf{K}\ \Delta\mathbf{u} = {}_0^2\mathbf{F}_{th} - {}_0^1\mathbf{F}\ , \tag{1}$$

where the left upper index indentifies the displacement configuration or increment number (0-*initial*, 1-*intermidiate actual*, 2-*unknown* configuration) in which the particular term is to be evaluated, the left bottom index describes the reference state. These indices are later either omitted or used only if necessarily. ${}_0^1\mathbf{K}$ is the tangent stiffness matrix; $\Delta\mathbf{u}$ stands for the displacements increment; ${}_0^2\mathbf{F}_{th}$ is the thermal load vector, which is a function of temperature stresses in the unknown configuration, ${}_0^1\mathbf{F}$ is the balanced force vector. The matrix ${}_0^1\mathbf{K}$ can be divided into the following parts:

$$ {}_0^1\mathbf{K} = {}_0^1\mathbf{K}_u + {}_0^1\mathbf{K}_g - {}_0^2\mathbf{K}_{g,th}\ , \tag{2}$$

where ${}_0^1\mathbf{K}_u$ is the tangent stiffness matrix depending on actual displacements, ${}_0^1\mathbf{K}_g$ is the geometrical stiffness matrix depending on the stress state, ${}_0^2\mathbf{K}_{g,th}$ is the thermal geometrical stiffness matrix, which depends on the thermal stresses in the unknown configuration.

The solution's accuracy of Eqn. (1) needs to be improved by Newton-Raphson iterations:

$$\mathbf{K}({}^2\mathbf{u}^{(i-1)})\delta\mathbf{u}^{(i)} = \mathbf{F}_{th}({}^2\mathbf{u}^{(i-1)}) - \mathbf{F}({}^2\mathbf{u}^{(i-1)}), \tag{3}$$

where the right upper index stands for the iteration number.
The increment of displacements and the displacement vector are consequently actualised:

$$\Delta\mathbf{u}^{(i)} = \Delta\mathbf{u}^{(i-1)} + \delta\mathbf{u}^{(i)}, \qquad {}^2\mathbf{u}^{(i)} = {}^2\mathbf{u}^{(i-1)} + \delta\mathbf{u}^{(i)} \tag{4}$$

The iterations are executed until the convergence criterion is achieved. In the present study this criterion is imposed on the displacements:

$$\left\|\delta\mathbf{u}^{(i)}\right\| < \varepsilon\left\|\Delta\mathbf{u}^{(i)}\right\|, \tag{5}$$

where ε is a tolerance value.

Among all known path following methods, i.e. the load control, the displacement control or the arc-length control algorithms, the most attractive strategy is the latter one, because of its robustness in the vicinity of limit points on equilibrium path.
In this method it is assumed, that the load value in the unknown configuration can be expressed in terms of the load parameter ${}^2\lambda$ and the reference load $\mathbf{F}_{th,ref}$:

$${}^2\mathbf{F} = {}^2\lambda\,\mathbf{F}_{th,ref} \tag{6}$$

One has to be aware of the fact, that since the thermal load vector depends on the thermal stresses, $\mathbf{F}_{th,ref}$ cannot be obtained just once at the beginning of the analysis and then simply multiplied by the load parameter in an each step, as it can be done in static load problems. Strictly, only the temperature value, which thermal stresses depends on, is simply scaled by ${}^2\lambda$. The authors use however the above formula (6) in order to shorten the notation. Moreover it must be stressed, that only if load control method is used during the analysis, the temperature geometrical stiffness matrix (2) can be evaluated exactly with respect to the thermal stresses in the unknown configuration. Since the arc-length technique is employed, the temperature level in the unknown configuration is unidentified and therefore one has to use the matrix evaluated in the last iteration:

$${}_0^2\mathbf{K}_{g,th} = {}_0^2\mathbf{K}_{g,th}^{(i-1)} \tag{7}$$

The arc-length strategy utilizes a mixed displacement-load constraint:

$$(\Delta\mathbf{u}^{(0)})^T\Delta\mathbf{u}^{(0)} + (\Delta\lambda^{(0)})^2 = ds^2, \tag{8}$$

which allows to obtain the first load parameter increment.
Substituting ${}^2\lambda\,\mathbf{F}_{th,ref}$ for $\mathbf{F}_{th}$ one transforms the equation (3) into a form:

$$\mathbf{K}({}^2\mathbf{u}^{(i-1)})\delta\mathbf{u}^{(i)} = \delta\lambda^{(i)}\mathbf{F}_{th,ref}({}^2\mathbf{u}^{(i-1)}) - \mathbf{J}({}^2\mathbf{u}^{(i-1)}) \tag{9}$$

with unbalanced loads given as:

$$\mathbf{J}({}^2\mathbf{u}^{(i-1)}) = ({}^1\lambda + \Delta\lambda^{(i-1)})\mathbf{F}_{th,ref}({}^2\mathbf{u}^{(i-1)}) - \mathbf{F}({}^2\mathbf{u}^{(i-1)}) \tag{10}$$

There exist several variants of arc-length control method, depending on the constraint equation introduced in the algorithm, see e.g. [3].

In the present work the Riks-Wempner-Ramm [10] arc-length path following method has been applied. The mixed constraint load-displacement equation consists here in introducing the normal-plane to the tangent-plane, which is updated in each iteration:

$$(\Delta\mathbf{u}^{(i-1)})^T\,\delta\mathbf{u}^{(i)} + \Delta\lambda^{(i-1)}\,\delta\lambda^{(i)} = 0. \tag{11}$$

Additionally, it is assumed that:

$$\delta\mathbf{u}^{(i)} = \delta\lambda^{(i)}\delta\mathbf{u}_R^{(i)} + \delta\mathbf{u}_J^{(i)}, \tag{12}$$

whereas the displacement increment corrections $\delta\mathbf{u}_R^{(i)}$ and $\delta\mathbf{u}_J^{(i)}$ are evaluated from system of two equations:

$$\begin{aligned}\mathbf{K}({}^2\mathbf{u}^{(i-1)})\delta\mathbf{u}_R^{(i)} &= \mathbf{F}_{th,ref}({}^2\mathbf{u}^{(i-1)}),\\ \mathbf{K}({}^2\mathbf{u}^{(i-1)})\delta\mathbf{u}_J^{(i)} &= \mathbf{J}({}^2\mathbf{u}^{(i-1)})\end{aligned} \tag{13}$$

The correction $\delta\lambda^{(i)}$ comes from:

$$\delta\lambda^{(i)} = \frac{(\Delta\mathbf{u}^{(i-1)})^T\,\delta\mathbf{u}_J^{(i)}}{(\Delta\mathbf{u}^{(i-1)})^T\,\delta\mathbf{u}_R^{(i)} + \Delta\lambda^{(i-1)}} \tag{14}$$

In view of the fact, that thermally loaded thin shells are very sensitive to the buckling, a proper choice of the unloading condition determining the sign of the load parameter increment $\Delta\lambda^{(0)}$ plays a crucial role. Several criteria are discussed in details in [6].

In the authors' FEM code two conditions are available: 1) the sign of the load parameter increment taken as being equal to the sign of the current stiffness matrix determinant:

$$sign(\Delta\lambda^{(0)}) = sign(|\mathbf{K}|)\,, \tag{15}$$

2) the sign of the load parameter increment determined by the direction of the previous increment [14]:

$$sign(\Delta\lambda^{(0)}) = sign((\Delta\mathbf{u})^T \delta\mathbf{u}_R + \Delta\lambda)\,, \tag{16}$$

where the values on the RHS of (16) correspond to the previous increment.

The first criterion (Eqn. (15)) works well in a case of the mechanical loading, however, for thermally loaded shells the second criterion (Eqn. (16)) is more suitable (see [14]).

4. Strength analysis

The information about the buckling load level is apparently inadequate, if the loss of stability occurs after a material failure. Thus, as mentioned before, it is reasonable to control the stress state in an every layer for the each converged displacement state. The load value, at which the material failure occurs for the first time is called the first-ply failure load [15]. From the practical point of view, if the analysis is carried out after the first material failure is detected, one should reduce the stiffness of the shell in the damaged regions. Such an approach is called a progressive failure analysis, see [9, 15]. The present study is limited to an estimation of the first-ply failure.

Generally, due to the orthotropy of layers and to various orientation of fibres in the stacking sequence, the stress state present in a laminate is relatively complex, even for simple load cases. Therefore, the choice of a proper strength criterion plays a crucial role. Several various strength criteria are available for multilayered composites, see [8, 15]. From the most popular ones, namely the maximum strain criterion, Hill criterion or Hoffman criterion, the most universal seems to be the Tsai-Wu hypothesis, which enables the analysis of materials with different tensile and compressive strengths. Moreover, the theoretical results obtained in terms of the Tsai-Wu criterion usually agree very well with the experimental data.

The failure surface of the Tsai-Wu criterion describes the following equation:

$$F_1\sigma_1 + F_2\sigma_2 + F_{11}\sigma_1^2 + F_{22}\sigma_2^2 + 2F_{12}\sigma_1\sigma_2 + F_3\sigma_{12}^2 = 1\,, \tag{17}$$

with polynomial coefficients:

$$\begin{aligned} &F_1 = \left(\frac{1}{X_t} - \frac{1}{X_c}\right); \qquad F_2 = \left(\frac{1}{Y_t} - \frac{1}{Y_c}\right); \\ &F_{11} = \frac{1}{X_t X_c}; \qquad F_{22} = \frac{1}{Y_t Y_c}; \qquad , \\ &F_{12} = \frac{-1}{2\sqrt{X_t X_c Y_t Y_c}}; \quad F_3 = \frac{1}{S^2}; \end{aligned} \tag{18}$$

where X_t, X_c are, respectively, the longitudinal tensile and compressive strength; Y_t, Y_c stand for the transverse tensile and compressive strength, correspondingly; S represents the shear strength of a layer; whereas σ_1, σ_2, σ_{12} symbolize stress components in the principal material coordinates. F_{12} denotes the factor of an interaction between σ_1 and σ_2 [8, 15]. Its value should be determined experimentally in a biaxial test. However, since such a procedure is a little bit complicated, usually F_{12} is set to zero or it is evaluated from the given formula (18), see [15, 18].

5. Examples and discussion

To illustrate the efficiency of the proposed numerical model, several examples are presented. The all described below computations have been performed with the use of an isoparametric variable node number (8 to 16) doubly-curved shell element [10].

5.1. Laminated plates

The first considered example is taken after the paper of Srikanth and Kumar [19], where the stability and the failure of multilayered plates in the uniform temperature field were analysed. The authors of [19] investigated the influence of the number of layers, the fibres arrangement and the temperature dependency of material data on the structure behaviour. In the present study a 16-layered square plate with temperature independent material characteristics is investigated for 3 stacking sequences: quasi-isotropic $[\pm 45/0/90]_{2s}$, cross-ply $[0/90]_{4s}$ and angle-ply $[\pm 45]_{4s}$. The aspect ratio a/h=100 (Fig.1), with h standing for the total thickness of the laminate. All layers are made of a material with the following parameters: E_1=141 GPa, E_2=13.1 GPa, $G_{12}=G_{13}=G_{23}$=9.31 GPa, ν_{12}=0.28, $\alpha_1=0.18\cdot10^{-6}$ 1/°C, $\alpha_2=21.8\cdot10^{-6}$ 1/°C, $X_t=X_c$=1650 MPa, Y_t=58.9 MPa, Y_c=236 MPa, S=106 MPa. The all four edges of the plate are simply supported.

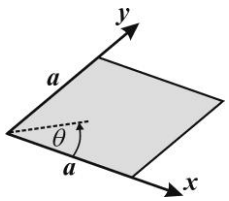

Figure 1: Geometry of square plate

The plate was divided into 8x8 8-node finite elements with uniformly reduced integration (8URI). Assuming the possible occurrence of a bifurcation point on the equilibrium path, in the first phase of the analysis the loading of the plate was disturbed by a small centrally situated transverse upward point force, which was removed beyond the path junction point. Figures 2-4 present equilibrium paths of the central deflection. As can be observed, they agree quite well with the reference solutions. The obtained buckling temperatures have values: 80˚C, 63˚C, and 84˚C, respectively, in the case of quasi-isotropic, cross-ply and angle-ply stacking sequence.

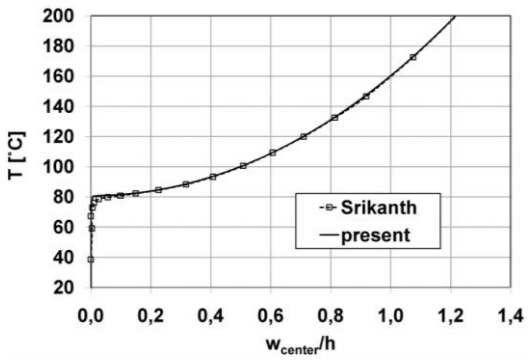

Figure 2: Quasi-isotropic square plate, equilibrium path of central deflection

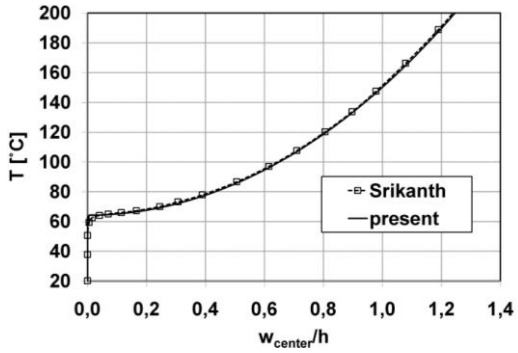

Figure 3: Cross-ply square plate, equilibrium path of central deflection

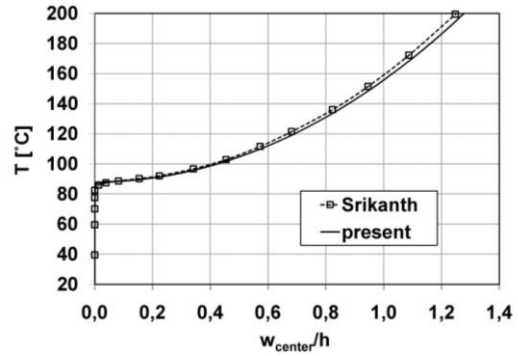

Figure 4: Angle-ply square plate, equilibrium path of central deflection

The strength analysis reveals that the first-ply failure temperature obtained from the Tsai-Wu criterion exceeds significantly the buckling temperature in all the considered cases of the fibre arrangements. The first failure occurs in the bottom layer as a consequence of matrix cracking in T=718 (700)˚C, T=810 (794.5)˚C, T=712 (691)˚C, correspondingly for $[\pm 45/0/90]_{2s}$, $[0/90]_{4s}$ and $[\pm 45]_{4s}$ lamination scheme. The values given in the brackets are the reference solutions [19]. It is remarkable, that the cross-ply plate represents the highest strength together with the worst buckling resistance, if compared with the angle-ply and the quasi-isotropic case.

5.2. Cylindrical orthotropic shell

This example has followed a proposal of Huang and Tauchert [7]. It has been already widely examined by other authors, e.g. [1, 12] and thus it can be treated as a popular benchmark problem for shells under uniform temperature rise.
A cylindrical one-layer orthotropic panel with following geometrical data $a=b=R\phi$, R/a=5, a/h=200, (Fig. 5) is investigated here. All edges are simply supported. The fibres are arranged in the circumferential direction (θ=90˚). The layer is made of the material with following data: E_1=138 GPa, E_2=8.28 GPa, $G_{12}=G_{13}=G_{23}$=6.9 GPa, ν_{12}=0.33, $\alpha_1=0.18\cdot10^{-6}$ 1/°C, $\alpha_2=27\cdot10^{-6}$ 1/°C, $X_t=X_c$=1263 MPa, Y_t=33.7 MPa, Y_c=207 MPa, S=57.3 MPa.

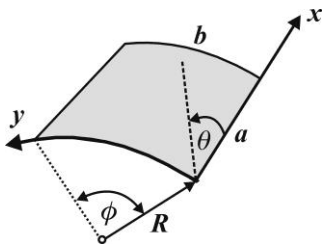

Figure 5: Geometry of cylindrical shell

In the present study, contrary to [1, 7, 12], the whole shell has been analysed. A uniform mesh of 16x16 8URI shell elements has been applied. The incremental analysis of the perfect structure with the use of condition given in Eqn. (16) leads to the same solution as obtained in [7] (Fig. 7, 8). However, while using condition (15) one can encounter some convergence problems about 80˚C, which are supposedly caused by a presence of a bifurcation point. To trace possible post-bifurcation paths, series of new computations were performed making use of condition (16) and applying small transverse load imperfections located at the points A, B, C, D, E, F shown in Fig. 6.

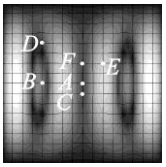

Figure 6: Locations of imperfections projected onto the deformation mode at 80˚C

Those small transverse perturbation forces were removed when the temperature rose above 80˚C. The imperfections applied at the points A or B have not changed the behaviour of the shell when compared with the perfect case. However, the disturbances introduced at points C or F (Fig. 7) and D or E (Fig. 8) have significantly influenced the structure response. The junction of paths in Fig. 7 appears about 82˚C, while in Fig. 8 it can be observed around 80˚C. Figure 9 shows the deflection shapes of the shell at the end of each path, i.e. in 100˚C.

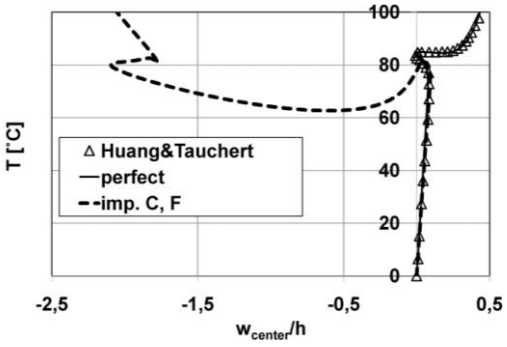

Figure 7: Equilibrium paths of orthotropic shell, primary path of perfect and imperfect shell (imperfections in points C, F)

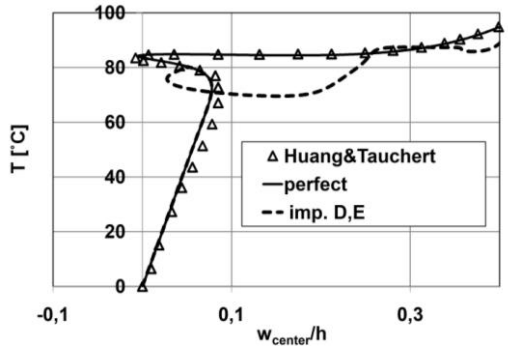

Figure 8: Equilibrium paths of orthotropic shell, primary path of perfect and imperfect shell (imperfections in points D, E)

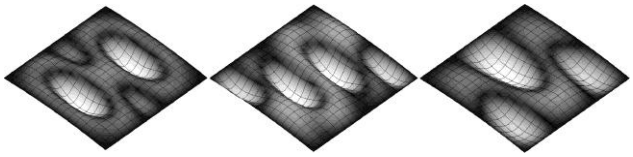

Figure 9: Deformation shapes at T=100˚C, a-perfect shell, b-imperfection in point D or E, c- imperfection in point C or F

Huang and Tauchert [7] reported that the first failure, according to the Tsai-Wu criterion, appeared on the primary path around 94˚C. It must be noticed that in [7] stresses were supposedly evaluated at nine Gauss points in each element. In the present analysis, stress values have been initially calculated at four Gauss points in each element and no failure occurred in the range 0˚C-100˚C. However, when the 8SRI element was applied in the present study, then due to a different location of the 'stress checkpoints', the failure temperature on the primary path would have a value of 96˚C. Nonetheless, one has to emphasized, that the best convergence of stress values in 8- and 9-node elements is achieved at points matching the Gauss points corresponding to the 2x2 integration scheme [20].

The allowable Tsai-Wu coefficient on the first secondary path (Fig. 8) is not exceeded up to 100˚C. On the other hand, on the second secondary path (Fig. 7) the failure occurs at 100˚C. However, regardless of the imperfection state, the snap-through phenomena takes place earlier than the material fails.

5.3. Cylindrical cross-ply shell

Oh and Lee [13] analysed an example of a simply supported cross-ply [0/90/90/0] cylindrical shell with the following geometrical data: $a=b=R\phi$, $\phi=15^{\circ}$ and various values of the ratio a/h (Fig. 5). The material properties are the same as in the previous section. In present work, the results for two cases are demonstrated: a/h=200 and a/h=800.

For the ratio a/h=200 the mesh of 10x10 8URI elements provides a sufficient mesh density. The symmetry conditions have not been applied in the current calculations. Figure 10 depicts equilibrium paths of the central deflection.

While using the condition (16) during the path's tracing of a perfect shell, the same solution as obtained by Oh&Lee is attained. On the other sight, the computations fail in the temperature of about 260˚C, if the condition (15) is employed. Supposing that the convergence problems are caused here by an arising of a bifurcation point, additional analyses were carried out with small transverse inward and outward load imperfections placed in several nodes. However, irrespective of a location and a direction of the imperfection, either a fundamental path or exactly the same secondary path were obtained (Fig.10). Thus only two points – A and C – are considered here, see Fig. 11. As one can observe the deformation shapes for two variants of imperfection are mutual reflections (Fig. 11), what may explain the coincidence of the secondary paths in Figure 10.

According to the Tsai-Wu criterion, no material failure were detected on the primary as well on the secondary path up to temperature of 400˚C.

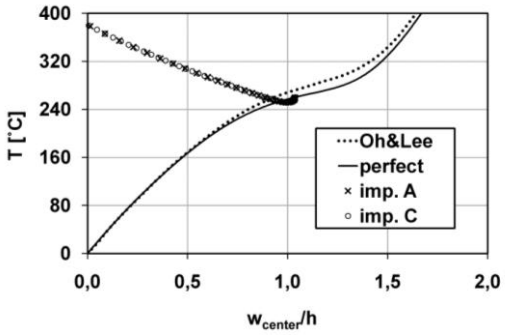

Figure 10: Cross-ply shell, a/h=200, fundamental and secondary paths

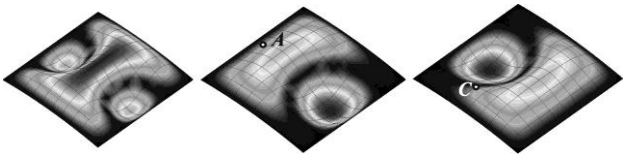

Figure 11: Shell a/h=200, deformation shapes at 400˚C: a - perfect shell, b - imperfection in point A, c - imperfection in point C

In the case of the shell with a/h=800, an attention should be paid to the proper element mesh density. Since the slenderness of the structure is significant, the appearance of shear locking during the computations can be expected.

Due to observed essential qualitative discrepancies between solutions obtained with 10x10 and 20x20 8URI elements in initial study of the convergence, an additional analysis were performed with the use of the 16FI (16-node element with full integration) element, which is generally free of locking phenomenon [10]. As shown in Fig. 12, the present solutions obtained with the 20x20 8URI and 14x14 16FI elements are compatible, whereas they disagree with the reference results [13], where a 10x10 mesh of layerwise, probably fully integrated 9-node elements were used. Further computations performed by the authors with the 9FI element (Fig. 13) showed, that the reference solution given in [13] can be very much influenced by the shear locking. Nevertheless, it must be mentioned, that this example is also presented in [12], where Reissner-Mindlin elements with independent strain field were employed. Surprisingly, the same results as in [13] were reported.

The stress-bearing capacity for this example investigated by means of the Tsai-Wu criterion has not indicated any failure in the range 0˚C-100˚C.

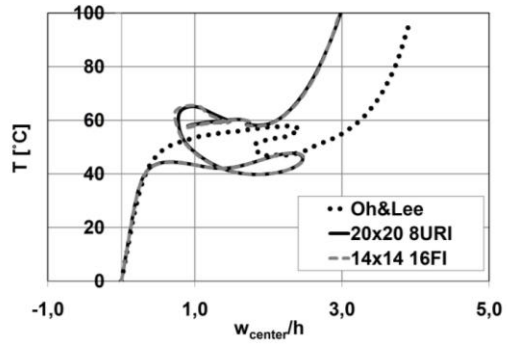

Figure 12: Cross-ply shell, 8URI and 16FI elements

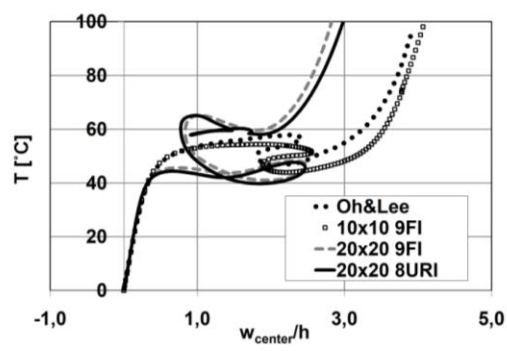

Figure 13: Cross-ply shell, 8URI and 9FI elements

6. Concluding remarks

This work presents the *Equivalent Single Layer* numerical model for an analysis of multilayered composite plates and shells subjected to a uniform thermal loading. The first order shear deformation theory established the basis of the presented approach. The aim of the paper was to determine the carrying capacity of the structure. Taking into account the sensitivity to instability of thermally loaded shells, the geometrically non-linear analysis were performed to find either the bifurcation or load limit points. For the completeness of the investigations, the stress state and a possible material failure was monitored in each increment of the analysis. The state of a material was treated as a safe one until the polynomial of the Tsai-Wu criterion was fulfilled. The following conclusions can be drawn:

- The agreement with reference results proves the efficiency of the proposed formulation;
- The choice of an appropriate unloading condition used in the arc-length algorithm is of a great importance;
- The carrying capacity of multilayered thin plates and shells is very often determined by the instability effects.

References

[1] Barut A., Madenci E. and Tessler A., Nonlinear thermoelastic analysis of composite panels under non-uniform temperature distribution, *Int. J. Solids Struct*, 37, pp. 3681-3713, 2000.

[2] Brank B. and Carrera E., Multilayered shell finite element with interlaminar continuous shear stresses: a refinement of the Reissner-Mindlin formulation, *Int. J. Numer. Meth. Engn*, 48, pp. 843-874, 2000.

[3] Carrera E., A study on arc-length-type methods and their operation failures illustrated by a simple model, *Comput. Struct.*, 50, pp. 217-229, 1994.

[4] Chróścielewski J., Pietraszkiewicz W. and Witkowski W., On shear correction factors in the non-linear theory of elastic shells, *Int. J. Solids Struct.*, 47, pp. 3537-3545, 2010.

[5] El Damatty A.A, Awad A.S. and Vickery B.J., Thermal analysis of FRP chimneys using consistent laminated shell element, *Thin Walled Struct.*, 37, pp. 57-76, 2000.

[6] Feng Y.T., Perić D. and Owen D.R.J, A new criterion for determination of initial loading parameter in arc-length methods, *Comput. Struct.*, 58, pp. 479-485, 1996.

[7] Huang N.N. and Tauchert T.R., Large deflections of laminated cylindrical and doubly-curved panels under thermal loading, *Comput. Struct.*, 41, pp. 303-312, 1991.

[8] Jones R.M., *Mechanics of composite materials, 2nd ed*. Taylor&Francis, USA, 1999.

[9] Knight N.F., Rankin C.C. and Brogan F.A., STAGS computational procedure for progressive failure analysis of laminated composite structures, *Int. J. Non Linear Mech.*, 37, pp. 833-849, 2002.

[10] Kreja I., *Geometrically non-linear analysis of layered composite plates and shells*, Wydawnictwo Politechniki Gdańskiej, Gdańsk, 2007.

[11] Kreja I., A literature review on computational models for laminated composite and sandwich panels, *Cent. Eur. J. Eng.*, 1, pp. 59-80, 2011.

[12] Lee J.J, Oh I.K., Lee I. and Yeom C.H., Thermal postbuckling behaviour of patched laminated panels under uniform and non-uniform temperature distributions, *Compos. Struct.*, 55, pp. 137-145, 2002.

[13] Oh I.-K. and Lee I., Thermal snapping and vibration characteristics of cylindrical composite panels using layerwise theory, *Compos. Struct.*, 51, pp. 49-61, 2001.

[14] Parente E. Jr, de Holanda A.S. and Afonso da Silva S.M.B., Tracing nonlinear equilibrium paths of structures subjected to thermal loading, *Comput. Mech.*, 38, pp. 505-520, 2006.

[15] Reddy J.N., *Mechanics of laminated composite plates and shells. Theory and analysis, 2nd ed.*, CRC Press, USA, 2004.

[16] Rohwer K., Friedrichs F. and Wehmeyer C., Analyzing laminated structures from fibre-reinforced material – an assessment, *Tech. Mech.*, 25, pp. 59-79, 2005.

[17] Sabik A. and Kreja I., Analysis of multilayered plates with the use of equivalent single layer models (in Polish), *Acta Mechanica et Automatica*, Vol. 2, No. 1, pp. 63-68, 2008.

[18] Sabik A. and Kreja I., Stability analysis of multilayered composite shells with cut-outs, *Archives of Civil and Mechanical Engineering*, 11, pp. 195-207, 2011.

[19] Srikanth G. and Kumar A., Postbuckling response and failure of symmetric laminates under uniform temperature rise, *Compos. Struct.*, No. 1, pp. 109-118, 2003.

[20] Vlachoutsis S., Shear correction factors for plates and shells, *Int. J. Num. Meth. Engng*, Vol. 33, pp. 1537-1552, 1992.

[21] Zhang X., Why do Barlow points not coincide with the reduced Gauss quadrature points for higher-order finite elements?, *Commun. Numer. Meth. Engng*, Vol. 24, pp. 1251–1256, 2008.